Agricultural Water Management 144 (2014) 140–149

Contents lists available at ScienceDirect

Agricultural Water Management

journal homepage: www.elsevier.com/locate/agwat

Temporal stability analysis for estimating spatial mean soil water storage and deep percolation in irrigated maize crops

Danfeng Li[a,c], Ming'an Shao[b,*]

[a] State Key Laboratory of Soil Erosion and Dryland Farming on the Loess Plateau, Institute of Soil and Water Conservation, Chinese Academy of Sciences and Ministry of Water Resources, Yangling 712100, Shaanxi, China
[b] State Key Laboratory of Soil Erosion and Dryland Farming on the Loess Plateau, Northwest A & F University, Yangling 712100, Shaanxi, China
[c] University of Chinese Academy of Sciences, Beijing 100049, China

ARTICLE INFO

Article history:
Received 9 March 2014
Accepted 23 May 2014
Available online 2 July 2014

Keywords:
Soil water balance
Temporal variability
Deep percolation
Evapotranspiration

ABSTRACT

The temporal stability of soil moisture in irrigated cropland may have profound implications for precision agriculture in arid regions. This study evaluated the temporal variation of components of the soil water balance in irrigated cropland in northwestern China and identified representative locations to reliably estimate the profiles (0–1 and 1–2 m) of spatial mean soil water storage (SWS) and deep percolation below a depth of 2 m. Soil water storages were determined with a neutron probe at 48 locations (31 and 17 in the northern and southern croplands, respectively) on a total of 18 occasions in 2011 and 2012. Crop evapotranspiration, SWS variations and deep percolation were analyzed during the maize growing seasons. Soil water storages in the northern and southern croplands were temporally stable. The location with the lowest standard deviation of relative differences could accurately estimate the spatial mean SWS with a high coefficient of determination ($R^2 > 0.91$, $P < 0.001$) and prediction accuracy (PE > 0.76) and near-zero mean absolute relative error (MARE = 0). The most representative locations were different for the 0–1 and 1–2 m soil layers, but the location for the 0–1 m layer could also generally represent SWS in the 1–2 m layer in the northern and southern croplands. From 21 May to late September in both years, approximately 39 and 22% of the irrigation and rainwater were lost as deep percolation in the northern and southern croplands, respectively. Deep percolation at the most representative locations of spatial mean SWS for the 0–1 m layers could generally estimate the spatial mean deep percolation below a depth of 2 m. This study provides an alternative approach for estimating spatial mean SWS and deep percolation, which is essential for the rational management of scarce resources of irrigation water in a large arid region of northwestern China.

1. Introduction

Information for the components of water balance under irrigated agriculture is crucial for planning irrigation and for exploring water-saving measures at field scales. Quantifying the portioning of irrigation water during the growing period is important for the development, soil water movement and the management of agricultural water (Ji et al., 2007). Precipitation and ice/snow melt from the Qilian Mountains along the Heihe River basin of northwestern China are the sole sources of water available for the entire basin (Wang and Cheng, 1999). As one of the main regions for the production of commodity grain in China, the middle basin consumes ~86% of the total volume of the surface runoff, and ~96% of the water consumed is used for agricultural irrigation (Chen et al., 2003). The drastic population growth and the increasing use of irrigation in the middle basin in recent decades have increased water deficits, which in turn have accelerated ecological degradation downstream (Chang et al., 2006). Irrigation using groundwater has thus become increasingly important for promoting agricultural productivity in the middle basin. A large amount of irrigation water, however, is depleted by severe evaporation and drainage below the root zone due to conventional flood irrigation (Chen et al., 2005; Ji et al., 2007). Popularizing water-conserving irrigation techniques is essential to alleviate the wastage of irrigation water in the middle basin (Wang and Cheng, 1999). One approach to reduce the wastage is to control deep percolation. Minimizing deep percolation may reduce the risk of a high groundwater table and the subsequent salinization of the root zone, and would be vital to the sustainability of irrigated agriculture (Tanji and Kielen, 2002).

* Corresponding author. Tel.: +86 29 87012245.
E-mail address: mashao@ms.iswc.ac.cn (M. Shao).

http://dx.doi.org/10.1016/j.agwat.2014.05.012
0378-3774/

The accurate estimation of crop evapotranspiration, changes in soil water storage (SWS) and deep percolation below the root zone can determine the proper scheduling of irrigation and provide a basis for improving the use efficiency of irrigation water (Li et al., 2003; Pereira et al., 2007; Ma et al., 2013). The spatial variability of SWS, however, presents a challenge for the scheduling of irrigation due to the difficulty in obtaining field averages (Van Pelt and Wierenga, 2001). Site-specific measurements with fine resolution in both space and time are time-consuming, costly and laborious. The analysis of temporal stability may be an alternative strategy to accurately estimate spatial mean SWS with reduced effort (Hu et al., 2012b). The concept of temporal stability was first proposed by Vachaud et al. (1985) and has received considerable attention in studies of soil moisture on various spatial scales in various climatic regions in recent decades (Pachepsky et al., 2005; Guber et al., 2008; Hu et al., 2014). The possible extrapolation of soil moisture data from a certain depth at one location to the entire soil profile at point or slope scales using the concept of temporal stability, has been recently explored by Hu and Si (2014). The study of the temporal stability of soil moisture in irrigated cropland has mostly focused on small fields (Starr, 2005; de Souza et al., 2011; Cosh et al., 2012), and the temporal stability in irrigated cropland larger than tens or thousands of hectares during the growing season is poorly known. The direct measurement of deep percolation is difficult, so modeling plays an increasingly important role in guiding experimentation and decision-making. Deep percolation is usually quantified based on soil water balance under different irrigation strategies for various crops (Moreno et al., 1996; Vázquez et al., 2006; Ji et al., 2007; Kang et al., 2012; Wang et al., 2012). The applicability of Richards' equation models in predicting deep percolation has also been evaluated (Stewart et al., 2006; Jiménez-Martínez et al., 2009; Sella et al., 2011). Richards' equation models, however, require various parameters of the crop and soil hydraulics, so previous studies have mostly focused on small croplands. A simple method for evaluating deep percolation during the growing season in cropland larger than tens or thousands of hectares could thus provide information for the determination of water-saving schedules of irrigation in arid regions.

It would be appealing if spatial mean SWS and deep percolation during the growing season could be predicted from measurements at very few locations. The use of a temporally stable pattern of SWS as a basis for the management of precision agriculture, however, has received little attention. A spatially variable but temporally stable pattern of application of irrigation water could save energy, labor and costs and could benefit the management of scarce resources of irrigation water in arid regions. Therefore, the objectives of this study were: (1) to analyze components of the soil water balance in irrigated maize cropland in an arid region of northwestern China, and (2) to evaluate the temporal patterns of both SWS and deep percolation during the growing periods of maize and identify the representative locations for adequately predicting the spatial means of SWS and deep percolation.

2. Materials and methods

2.1. Study area

The study was conducted at the Linze Inland River Basin Comprehensive Research Station of the Cold and Arid Region Environment and Engineering Institute, Chinese Academy of Sciences. This region is in the middle part of the Heihe River basin in northwestern China and is characterized by desert with fixed or semi-fixed sand dunes, cropland in patchily distributed oases and wetland with severely salinized soil surfaces (Fig. 1). The region has a continental, dry, temperate climate with a mean annual air temperature of 7.6 °C. Mean annual precipitation is 120 mm, ~60% of which falls from July to September, while only 3% falls during winter. The mean annual potential evaporation is 2360 mm, and the drying index is 15.9 (Zhao et al., 2010). Each year has ~165 frost-free days. The growing period ranges from March to October. Agriculture relies on conventional flood irrigation sourced from groundwater (Chen et al., 2005; Ji et al., 2007). The desert vegetation in the northern and middle parts of the study area consists of *Halaxylon ammodendron* (C. A. Mey.) Bunge, *Calligonum mongolicum* Turcz., *Tamarix chinensis* Lour., *Nitraria sphaerocarpa* Maxim and *Reaumuria soongorica* (Pall.) Maxim. The predominant species in the wetland are Common Reed (*Phragmites australis* (Cav.) Trin. ex Steud.), Common Leymus (*Leymus secalinus* (Georgi) Tzvel.), *Achnatherum splendens* (Trin.) Nevski, *Kalidium foliatum* (Pall.) Moq. and *N. tangutorum* Bobr. Soils in the northern and southern parts of the study area differ both in the vertical and horizontal directions (Li and Shao, 2013). The zonal soil in the northern margin of irrigated cropland is an Aridisol derived from diluvial–alluvial materials (Su et al., 2010). Siltigi-Orthic Anthrosols have developed under long-term irrigation from sediment-rich water, fertilization and cultivation in the central and southern parts of the study area (Su et al., 2009). The wetland in the southern part of the study area has Inceptisols.

Maize (*Zea mays* L.) for seed production is the staple crop in the study area. The growing period was 155 days from sowing to harvest. Field observations were conducted from germination to harvest. The growing period was divided into four phenological stages: initial, development, mid-season and late season of 30, 50, 42 and 33 days, respectively (Zhao et al., 2010). The maize in the northern cropland was sown on 9–10 and 14–15 April in 2011 and 2012, respectively, and harvested on 11–12 and 14–15 September in 2011 and 2012, respectively. Soil water content was considerably high in the southern cropland, so the spring thaw of frozen soil was later in the southern than in the northern cropland. To facilitate the mechanical operations before sowing and to guarantee germination by avoiding seed mildew and rotting, the sowing and subsequent growing stages in the southern cropland were 15 days later than those in the northern cropland. The groundwater level was shallower in the southern than in the northern cropland. In addition, the differences in soil texture led to different capacities of soil water retention in the northern and southern croplands. The fine-textured soil in the southern cropland was able to hold more water than the coarse-textured soil in the northern cropland. The maize was thus irrigated seven times with 120 mm of water (at 15–17 day intervals) in the northern cropland and four times with 150 mm of water (once a month) in the southern cropland during the growing seasons. The croplands were plowed after harvest in September and kept bare throughout the winter and were irrigated with 150 mm of water sourced from the Heihe River in mid-November of both years to maintain soil moisture.

2.2. Sampling and measurement

Previous studies have shown that roots of maize even can reach to a depth of 2 m (Teare and Peet, 1983; Liu et al., 2009). Therefore, we focused on the temporal variation of components of soil water balance in the 0–2 m soil profile during the growing season in this study.

2.2.1. Measurement of soil moisture

A total of 48 aluminum neutron-probe access tubes were installed at a depth of 3 m in the croplands in April 2011 (Fig. 1), 31 and 17 in the northern and southern parts of the study area, respectively. Volumetric soil water contents (θ, $cm^3\,cm^{-3}$) were determined with a neutron probe at the 48 locations, and the piecewise-constant rule (at 0.1- and 0.2-m intervals for the 0–1

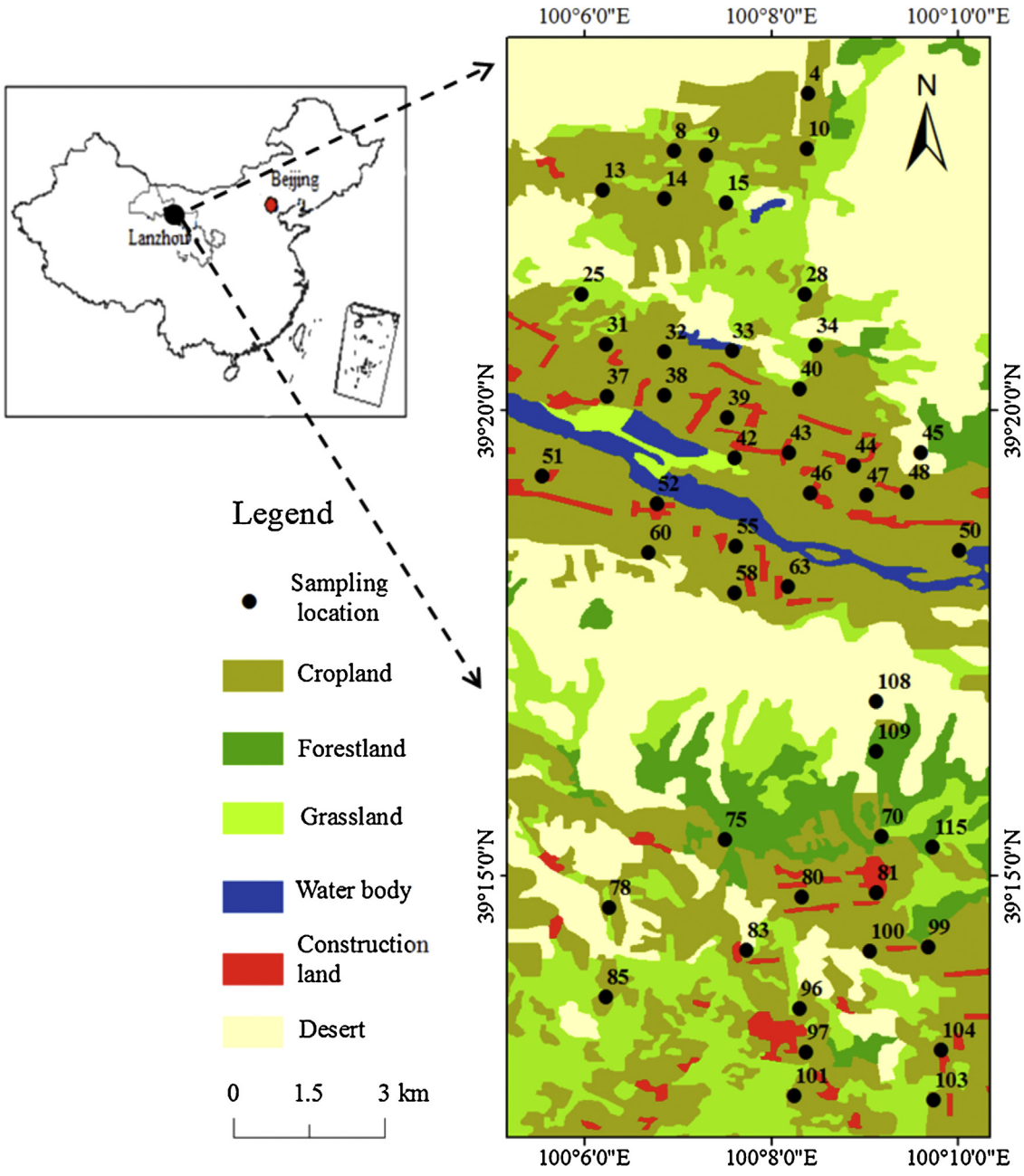

Fig. 1. The location of the study area in China and sampling locations in the study area.

and 1–2 m soil layers, respectively) was applied. Some access tubes were eroded by salts below the 1-m layer, so measurements for the 1–2 m layer at these locations were collected on fewer than 18 occasions. Measurements for the 1–2 m layer at only 27 of the 31 locations in the northern cropland and 15 of the 17 locations in the southern cropland were thus analyzed in this study. The measurements were conducted regularly once a month from May to October in 2011, in December 2011 and from February to December in 2012, for a total of 18 occasions. The measurements for each occasion were completed within three days. The measurements in May of both years were conducted four days before the first irrigation after sowing, and the following three occasions (June–August) were five days after irrigation. The measurements in September of both years were conducted about twenty days after the irrigation in August. Measurements outside the growing season were conducted regularly in the third week of each month. Soil water storage (mm) for location i at time j, $SWS_{i,j}$, in the 0–1 or 1–2 m layers, was calculated from $\theta(i,j,k)$ (where k is soil depth, m) using the following trapezoidal rules:

$$SWS_{i,j}(0-1\,\text{m}) = [\theta(i,j,0.1) + \theta(i,j,0.2) + \cdots + \theta(i,j,1.0)] \times 100$$
$$SWS_{i,j}(1-2\,\text{m}) = [\theta(i,j,1.2) + \theta(i,j,1.4) + \cdots + \theta(i,j,2.0)] \times 200 \quad (1)$$

2.2.2. Measurement of meteorological factors

The meteorological variables were monitored by a standard automated weather station installed at the research station. Precipitation, air temperature, humidity, vapor pressure, solar radiation and wind speed were recorded hourly. The meteorological data for 2011 and 2012 are presented in Fig. 2. The total rainfalls were 101.4 and 106.2 mm in 2011 and 2012, respectively, 98.2 and 97.6%

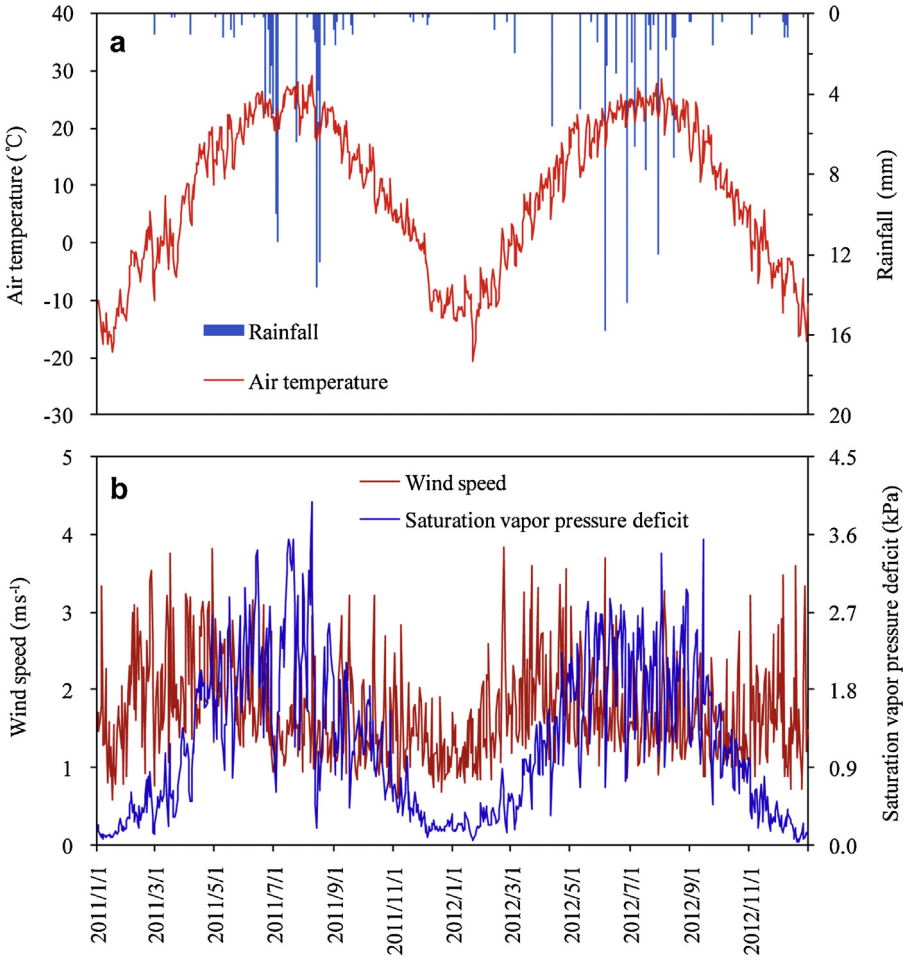

Fig. 2. Meteorological factors in the study area in 2011 and 2012.

of which, respectively, were recorded during the growing periods (Fig. 2a). The highest and lowest mean daily air temperatures were in August and January, respectively (Fig. 2a). The mean annual wind speed was 1.73 m s^{-1} (Fig. 2b). In both years, the saturation vapor-pressure deficit increased from January, peaked in autumn and then decreased (Fig. 2b).

2.2.3. Measurement of other soil properties

A differential GPS receiver with an accuracy of 3–5 m was used to record the position of each location. The distributions of particle size and concentrations of organic carbon for the soils have been reported in detail elsewhere (Li and Shao, 2013, 2014). A pit 1 m in depth was excavated at each location 0.5 m from the access tube to obtain samples of undisturbed soil for measuring saturated hydraulic conductivity (K_s, mm min^{-1}) using the constant-head method (Klute and Dirksen, 1986; Hu et al., 2012a). The soil columns were then oven-dried at 105 °C for 24 h to measure soil bulk density (BD, g cm^{-3}) using the dry weight of each column (Hu et al., 2012a). The selected soil and hydraulic properties in the 0–1 and 1–2 m layers of the northern and southern croplands are listed in Table 1.

2.3. Analysis of data

2.3.1. The temporal stability analysis

The relative difference analysis was applied to evaluate temporal stability. The relative difference, $\delta_{i,j}$, between SWS at location i and time j, $SWS_{i,j}$ and the spatial mean SWS at the same time, $\overline{SWS_j}$, was defined as (Vachaud et al., 1985):

$$\delta_{i,j} = \frac{SWS_{i,j} - \overline{SWS_j}}{\overline{SWS_j}} \quad (2)$$

The mean relative difference for each location, $\overline{\delta_i}$, and the standard deviation of the relative differences, $\sigma(\delta_i)$, over the measurement period were calculated by:

$$\overline{\delta_i} = \frac{1}{m}\sum_{j=1}^{m}\delta_{i,j} \quad (3)$$

$$\sigma(\delta_i) = \sqrt{\frac{1}{m-1}\sum_{j=1}^{m}(\delta_{i,j} - \overline{\delta_i})^2} \quad (4)$$

where m is the number of occasions of measurement. Relative difference analysis identifies locations that consistently overestimate ($\overline{\delta_i} > 0$), underestimate ($\overline{\delta_i} < 0$) or approach ($\overline{\delta_i} \approx 0$) the spatial mean SWS over time. $\sigma(\delta_i)$ characterizes the temporal variability of $\delta_{i,j}$. The location with the lowest $\sigma(\delta_i)$ is regarded as the most stable over time (Grayson and Western, 1998; Hu et al., 2010b).

A representative location is defined as the location where the measured SWS is either close to $\overline{SWS_j}$ or can obtain $\overline{SWS_j}$ after easy transformation (Vanderlinden et al., 2012). The simplest method to identify a representative location is to select the location with the $|\overline{\delta_i}|$ closest to zero and a low $\sigma(\delta_i)$ (Vachaud et al., 1985). Soil water storage at such a location mostly approximates to $\overline{SWS_j}$, but

Table 1
Descriptive statistics of selected soil properties in the northern and southern croplands in the study area.

Depth (m)	Statistics[a]	North (N = 31)[b]						South (N = 17)					
		Clay (%)	Sand (%)	SOC (g kg^{-1})	BD (g cm^{-3})	K_s (mm min^{-1})	n	Clay (%)	Sand (%)	SOC (g kg^{-1})	BD (g cm^{-3})	K_s (mm min^{-1})	n
0	Min	3.59	9.82	0.81	1.42	0.06	0.37	13.4	13.1	2.44	1.23	0.03	0.37
−1	Max	39.3	92.3	7.21	1.66	2.50	0.46	40.2	65.2	13.1	1.67	1.53	0.53
	Mean	23.3	43.6	3.63	1.53	0.79	0.42	32.2	25.6	5.44	1.49	0.54	0.44
	CV (%)	45.8	54.2	49.2	6.0	120.6	8.2	20.9	54.6	51.1	10.0	97.4	12.8
1	Min	0.98	3.57	0.75	–	–	–	4.39	4.20	0.82	–	–	–
−2	Max	56.4	95.6	7.80	–	–	–	50.1	88.2	4.66	–	–	–
	Mean	25.1	37.6	2.86	–	–	–	28.5	33.5	2.44	–	–	–
	CV (%)	54.5	75.5	56.9	–	–	–	43.9	81.5	44.0	–	–	–

[a] Min, minimum; Max, maximum; CV, coefficient of variation. All statistics were based on the mean values of diverse soil layers.
[b] N, sample number; SOC, soil organic carbon concentration; BD, bulk density; K_s, saturated hydraulic conductivity; n, the total porosity (n = 1 − BD/2.65); –, data do not exist.

it may be not the most stable due to the inherent error in $\sigma(\delta_i)$ (Hu et al., 2010b). The most stable location may produce a more precise estimation after providing an offset, because bias is potentially correctable whereas standard deviation is not (Schneider et al., 2008). $\overline{SWS_j}$ can be estimated indirectly by providing an offset of $\overline{\delta_i}$ to the SWS of the most stable location, SWS_i, (Grayson and Western, 1998) and can be expressed as:

$$\overline{SWS_j} = \frac{SWS_i}{1 + \overline{\delta_i}} \tag{5}$$

The location with the minimum $\sigma(\delta_i)$ was selected to identify the most representative location using the method of Grayson and Western (1998) in this study.

2.3.2. Soil water balance

The FAO Penman–Monteith model is recommended as the standard method for defining and computing the reference evapotranspiration, ET_0 (mm day^{-1}). The model calculates daily ET_0 as (Allen et al., 1998):

$$ET_0 = \frac{0.408\Delta(R_n - G) + \gamma(900/(T + 273))u_2(e_s - e_a)}{\Delta + \gamma(1 + 0.34u_2)} \tag{6}$$

where R_n is the net radiation at the crop surface (MJ m^{-2} day^{-1}), G is the soil heat flux density (MJ m^{-2} day^{-1}), T is the mean daily air temperature at a height of 2 m (°C), u_2 is the wind speed at a height of 2 m (m s^{-1}), e_s is the saturation vapor pressure (kPa), e_a is the actual vapor pressure (kPa), $e_s - e_a$ is the saturation vapor-pressure deficit (kPa), Δ is the slope of the vapor-pressure curve (kPa °C^{-1}) and γ is the psychrometric constant (kPa °C^{-1}).

The crop evapotranspiration, ET_c (mm day^{-1}), was determined using the single-crop coefficient, K_c (dimensionless), as (Allen et al., 1998):

$$ET_c = K_c ET_0 \tag{7}$$

The single crop coefficient is relevant and convenient for most studies of hydrological water balance and for planning and managing basic irrigation schedules. The values of K_c recommended by Allen et al. (1998) were adjusted in this study with meteorological data to produce values of 0.27, 1.15 and 0.60 for the initial, mid-season and late-season stages, respectively, of the maize crops.

Downward drainage (deep percolation) below the root zone can be calculated according to the soil water balance (Allen et al., 1998):

$$DP = r + I + \Delta SWS + W_g - ET_c - R \tag{8}$$

where DP is the deep percolation (mm), r is the rainfall (mm), I is irrigation (mm), ΔSWS is the calculated change in SWS in the 0–2 m layer (mm), R is the surface runoff (mm), W_g is the capillary rise from groundwater (mm). W_g was negligible because the water table was lower than 3.5 m during the growing period (Ji et al., 2007). R was neglected because the study area was flat. Positive values of DP indicate downward percolation below the root zone, whereas negative values indicate upward capillary action from lower layers to the root zone.

2.4. Statistical test

Three statistical variables evaluated the ability of representative locations to estimate the spatial mean SWS and deep percolation: the coefficient of determination (R^2), the mean absolute relative error (MARE) and the prediction accuracy (PE) (Panigrahi and Panda, 2003). The latter two variables were calculated as:

$$MARE = \frac{1}{m}\sum_{i=1}^{m}\frac{V_{io} - V_{ip}}{V_{io}} \tag{9}$$

$$PE = 1 - \frac{\sum_{i=1}^{m}(V_{io} - V_{ip})^2}{\sum_{i=1}^{m}(V_{io} - \overline{V_o})^2} \tag{10}$$

where m is the number of occasions of measurement, V_{io} is the spatial mean SWS (or spatial mean deep percolation) measured on individual occasions, V_{ip} is the SWS after offset (or deep percolation) at the most representative location on individual occasions of measurement, and $\overline{V_o}$ is the temporal average of spatial mean SWS (or spatial mean deep percolation) over the 18 occasions.

3. Results and discussion

3.1. Crop evapotranspiration

Crop evapotranspiration varied with the meteorological conditions and the growing stages of the maize (Fig. 3). The total ET_c values during the 2011 and 2012 growing seasons averaged 661.4 and 630.3 mm in the northern and southern croplands, respectively. These values were similar to those of 618.3 (Zhao et al., 2010) and 591.3 mm (Liu et al., 2010) for maize in the same northern region. The mean daily values of ET_c were 4.3 and 4.1 mm day^{-1} in the northern and southern croplands, respectively, which were similar to the values reported for the same region (Zhao et al., 2010) and for semi-arid north China (Li et al., 2003).

3.2. Temporal variations of SWS and associated spatial variability

The temporal trends of spatial mean SWS and the spatial variability of SWS during the period of measurement are presented in Fig. 4. The 1–2 m layer consistently stored more water than the

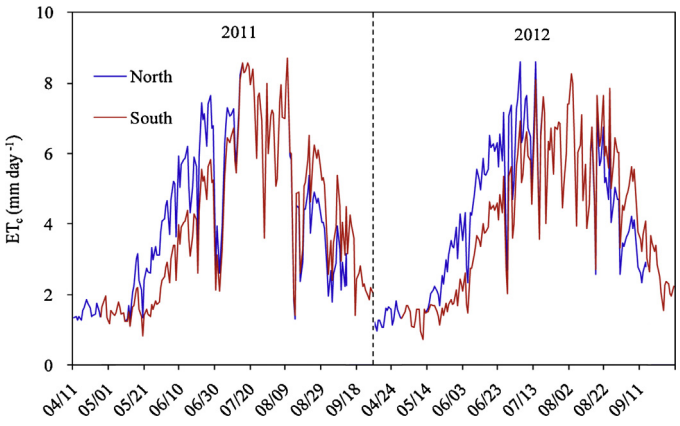

Fig. 3. Crop evapotranspiration in the northern and southern croplands during the growing periods in 2011 and 2012.

0–1 m layer in both the northern and southern croplands (Fig. 4a and b). The strong atmospheric demand of evapotranspiration depleted a large amount of water in the 0–1 m layer. The allocation of water to roots, though, can account for the difference in SWS between the 0–1 and 1–2 m layers. Approximately 95% of the maize roots were distributed in the 0–0.6 m soil layer, less than 2% were allocated below 0.8 m, and much less roots extended below 1.2 m (Zhou et al., 2008). Water uptake by roots contributed substantially to the depletion of water in the 0–1 m layer.

The temporal averages of spatial mean SWS in the northern cropland were 241.8 and 306.2 mm in the 0–1 and 1–2 m layers, respectively. The corresponding values were 269.0 and 329.2 mm, respectively, in the southern cropland. The temporal variability of spatial mean SWS was higher in the 0–1 m layer (coefficients of variation (CVs) of 9.5 and 6.6% in the northern and southern croplands, respectively) than in the 1–2 m layer (CV = 5.8 and 5.5% in the northern and southern croplands, respectively) (Fig. 4a and b). The seasonal change in meteorological conditions and the growth of maize were responsible for the large temporal variations in evapotranspiration and SWS in the 0–1 m layer. The lateral redistribution of soil moisture may also account for the temporal evolution of the SWS pattern in the 0–1 m layer (Penna et al., 2013). Water stored in the deeper layers tended to be more stable over time due to the absence of impacts from climate and agricultural management and the lack of water uptake by the roots (Choi and Jacobs, 2007; Hu et al., 2010a).

The spatial variability of SWS was higher in the 0–1 m layer than in the 1–2 m layer in the northern cropland during the period of measurement (Fig. 4c), whereas the opposite trend was observed in the southern cropland (Fig. 4d). The sand contents at locations 81 and 108 in the 1–2 m layer of the southern cropland were 70.4 and 76.7%, respectively, which were considerably higher than the mean of 33.5% for all locations (Table 1). The water-holding capacities were lower at these two locations than at other locations. Locations 81 and 108 were consistently drier than the other thirteen locations in the 1–2 m layer of the southern cropland over the 18 occasions of measurement. The mean SWS of the other thirteen locations ranged from 338.1 to 417.3 mm over the 18 occasions of measurement, with a temporal average of 375.9 mm, and the CVs of SWS ranged from 15.0 to 22.0%. The mean SWS at locations 81 and 108 varied from 106.5 to 165.3 mm over the 18 occasions of measurement, with a temporal average of 130.4 mm. The difference in the water-holding capacity due to the differences of soil texture among locations increased the spatial variability of SWS in the 1–2 m layer of the southern cropland. The spatial variability of SWS was more stable over time in the 1–2 m layer (CV = 6.9 and 5.2% in the northern and southern croplands, respectively) than in the 0–1 m layer (CV = 7.1 and 14.2% in the northern and southern croplands, respectively) during the period of measurement (Fig. 4 c and d). This result indicated a decreasing temporal variability in the spatial pattern of SWS with depth. The absence of disturbance by management practices, animals and the activities of roots may

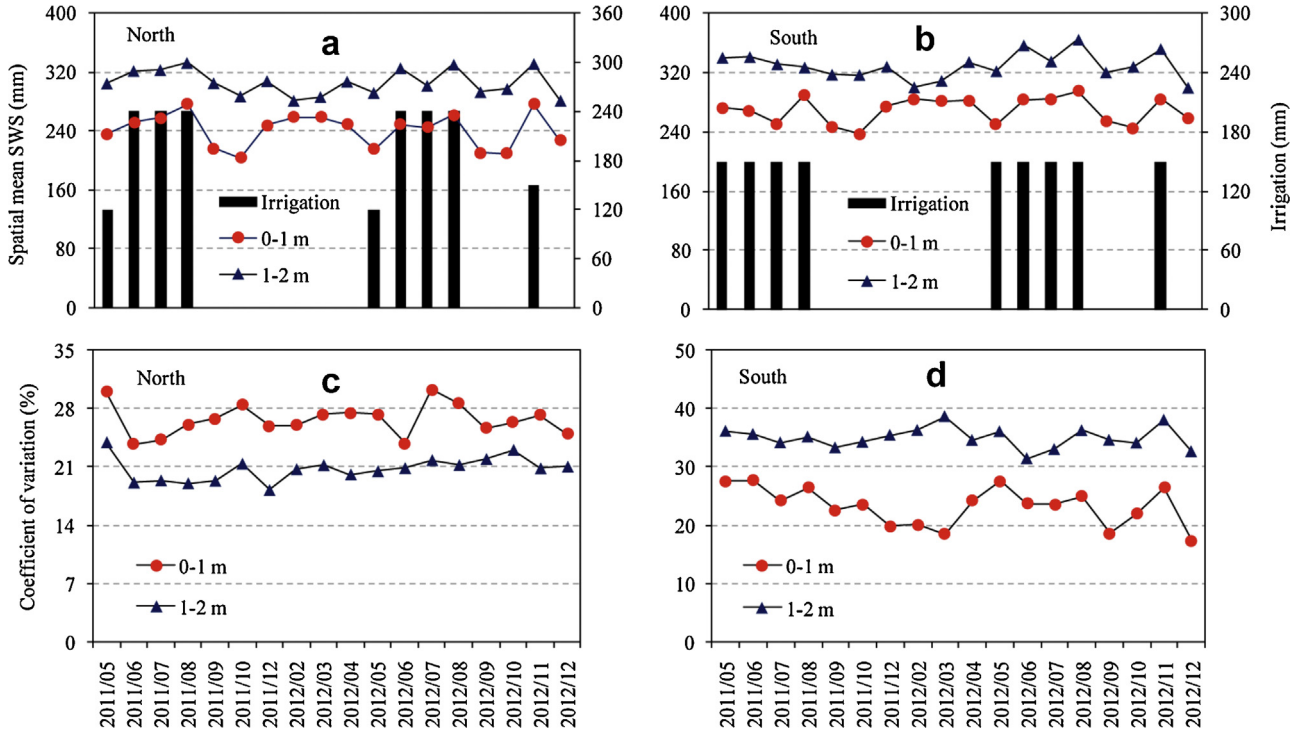

Fig. 4. The temporal trends of spatial mean soil water storage (a and b) and associated spatial variability (c and d) in the northern and southern croplands over the 18 occasions of measurement.

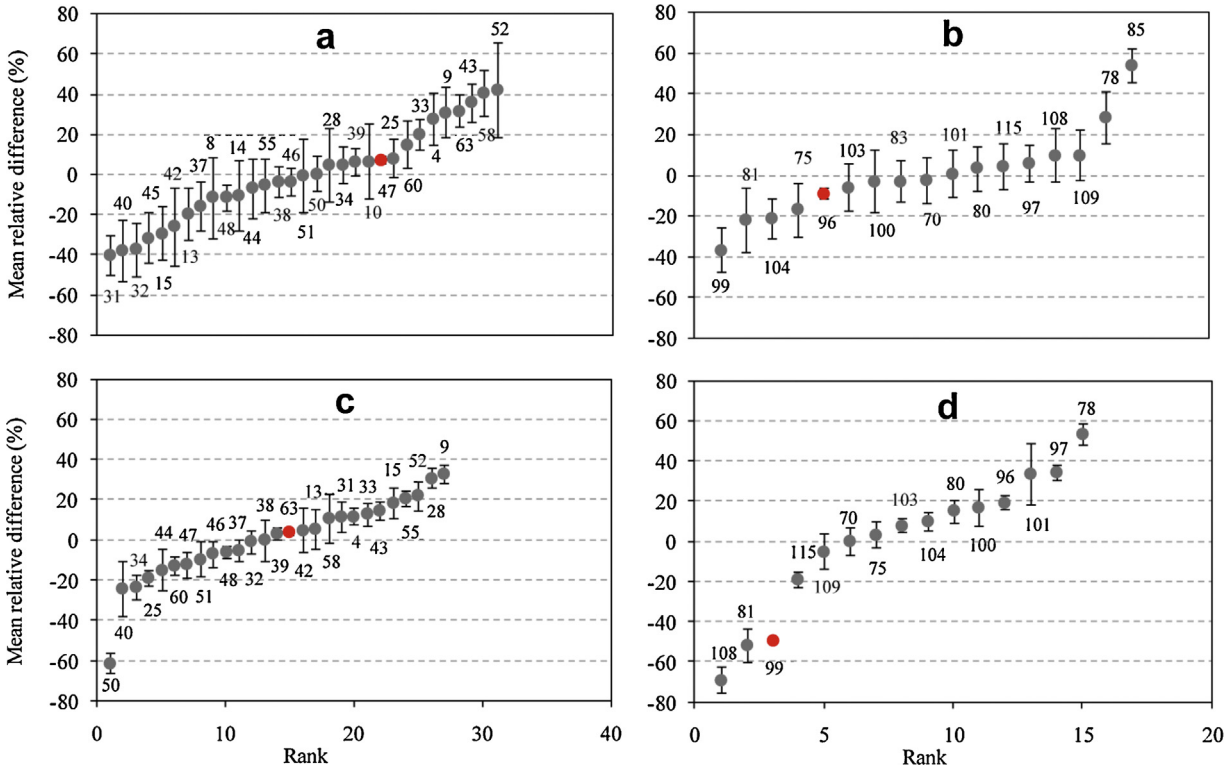

Fig. 5. Ranked mean relative differences of soil water storage in the 0–1 and 1–2 m layers in the northern (a and c, respectively) and southern (b and d, respectively) croplands. Values above or below the bars are the location numbers. Standard error bars correspond to ± one standard deviation of the relative differences. The most stable locations were marked in red color. (For interpretation of the references to color in this figure legend, the reader is referred to the web version of the article.)

account for the temporal persistence of the SWS spatial pattern in the 1–2 m layer.

3.3. Temporal stability of SWS

The ranked $\overline{\delta_i} \pm \sigma(\delta_i)$ of SWS in the 0–1 and 1–2 m layers of the northern and southern croplands are shown in Fig. 5. The range, maximum and minimum of $\overline{\delta_i}$ in the 0–1 and 1–2 m layers were lower in the northern (Fig. 5a and c) than the southern cropland (Fig. 5b and d). This result indicated that SWS in the northern cropland was more homogeneously distributed over space during the period of measurement. The most stable locations in the 0–1 and 1–2 m layers in the northern cropland were slightly wetter than the field averages ($\overline{\delta_i} = 7.3$ and 4.0%, respectively, Fig. 5a and c). The most stable locations in the 0–1 and 1–2 m layers in the southern cropland were relatively drier than the field averages ($\overline{\delta_i} = -8.7$ and −49.5%, respectively, Fig. 5b and d). Pearson correlation analysis showed that $\overline{\delta_i}$ and $\sigma(\delta_i)$ were negatively correlated in the 0–1 and 1–2 m layers of the northern cropland and in the 0–1 m layer of the southern cropland. $\overline{\delta_i}$ was positively correlated with $\sigma(\delta_i)$ in the 1–2 m layer of the southern cropland. These correlations, however, were not significant. High temporal stabilities of soil moisture in dry soils have been extensively reported (Martínez-Fernández and Ceballos, 2003; Jacobs et al., 2004; Cosh et al., 2008). In contrast, Guber et al. (2008) found no dependence of temporal stability on the average water content at a particular location. The relationship between temporal stability and the condition of the soil water depends on the criteria used. For standard deviation of relative differences, drier soils corresponded to stronger temporal stability, but the index of mean absolute bias error indicated the opposite trend (Hu et al., 2010b). Differences in soil properties and hydrological factors may account for the conflicting findings in different study regions. The near-zero MARE and the high R^2 and PE indicated that the most stable location, provided with an offset of $\overline{\delta_i}$, could accurately estimate the spatial mean SWS in each layer during the period of measurement (Fig. 6). These locations were regarded as the most representative. This result concurs with reports in the international literature. Starks et al. (2006) and Zhang and Shao (2013) found that locations with the minimum $\sigma(\delta_i)$ after offset gave the best estimates of the spatial mean soil water content. The most representative locations in our study were not identical in the two layers for either the northern or southern croplands, which was consistent with previous reports (Guber et al., 2008; Martinez et al., 2013). Representative locations 47 ($R^2 = 0.31$; MARE = 0.12) and 96 ($R^2 = 0.78$; MARE = −0.19) in the 0–1 m layers of the northern and southern croplands, respectively, however, could also generally estimate the spatial mean SWSs in the corresponding 1–2 m layers. Starks et al. (2006) also found that the stable dry or wet locations could represent various layers.

3.4. Deep percolation during the growing period

The temporal variations of deep percolation and the percentage of deep percolation of irrigation and rainwater from May to September in the two monitored years are presented in Fig. 7. Deep percolation from 21 May to late September averaged 330 mm over the two years in the northern cropland, representing ~39% of the irrigation and rainfall, and averaged 133 mm in the southern cropland, representing ~22% of the irrigation and rainfall. These percentages were lower than the 43% of the 840 mm irrigation water reported for the growing period of spring wheat in the northern cropland (Ji et al., 2007). Deep percolation was relatively high during the periods from 21 May to 20 June and 21 August to late September in 2011 and 2012 in both the northern and southern croplands (Fig. 7a). The amounts of deep percolation in the northern cropland from 21 May to 20 June represented 37.9 and 38.3% of

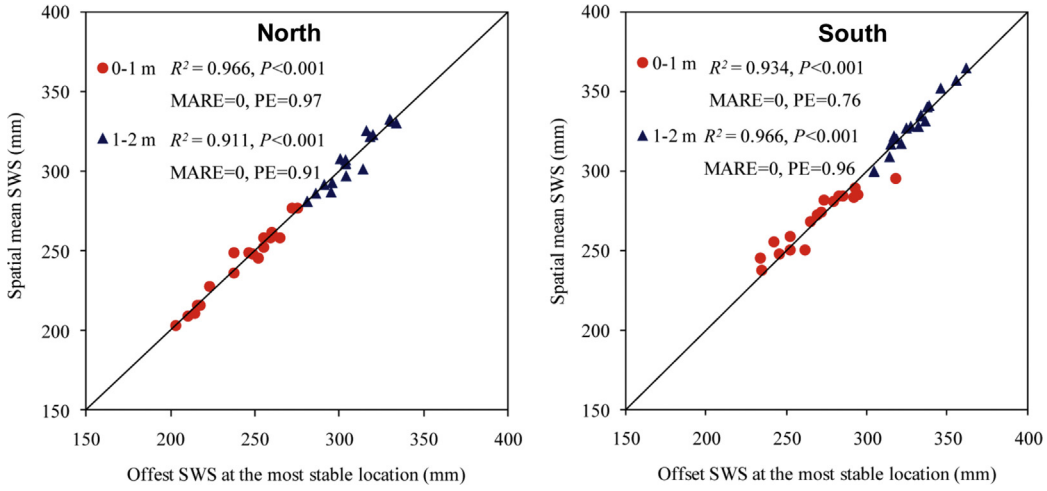

Fig. 6. The comparison of soil water storage at the most representative location to the spatial mean soil water storage in the northern and southern croplands.

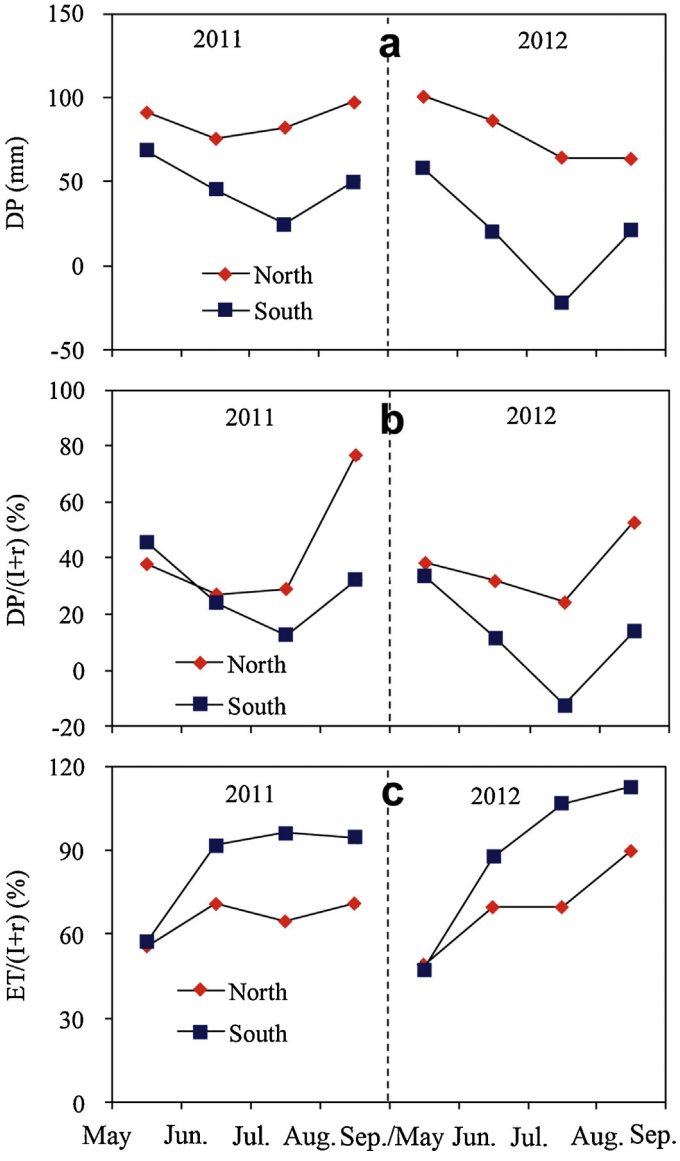

Fig. 7. The temporal variations of deep percolation (DP) (a) and the percentages of deep percolation and evapotranspiration (ET) of irrigation and rainfall ($I+r$) (b and c, respectively) in the northern and southern croplands during the growing periods in 2011 and 2012.

the irrigation and rainfall in 2011 and 2012, respectively. The corresponding values were 45.4 and 33.6% in the southern cropland (Fig. 7b). This period was in the initial and development stages of maize. Evapotranspiration gradually increased with the increasing leaf area index, a sufficient water supply satisfied the requirements of the crops, and excess water was lost by drainage below the root zone (Ma et al., 2013). The period from 21 August to late September was the late-season stage, when leaves began to senesce and less water was required. The percentages of deep percolation of irrigation and rainwater during this period in 2011 and 2012 were 76.8 and 52.7% in the northern cropland and 32.1 and 13.8% in the southern cropland, respectively (Fig. 7b). The temporal mean percentages in the late-season stage were 64.8 and 23.0% in the northern and southern croplands, respectively. For spring wheat in the northern cropland, deep percolation represented 46% of the irrigation and rainfall in the senescence stage (Ji et al., 2007). The last irrigation applied 15–20 days before harvest did not therefore efficiently benefit production in the northern cropland. The lower amount of percolation in the southern cropland may have been due to the delayed growing season and relatively stronger water holding capacity. The soil in the southern cropland was much finer-textured than the soil in the northern cropland (Li and Shao, 2013), so the water-holding capacity was higher in the southern cropland, and less water was lost by drainage than in the northern cropland.

The root zone in the southern cropland was recharged by capillary rise from the soil below 2 m in August and September of 2012 (Fig. 7a). Deep percolation from 21 June to 30 September in 2011 was low, and evapotranspiration represented more than 90% of the irrigation and rainfall. Even the recharge from the lower layers was consumed by the high evapotranspiration demand during this period in 2012 (Fig. 7c). Drainage dominated from the sowing to the heading stages of maize, while the soil water flux at the bottom of the root zone was mainly upward through capillary rise from the heading to the harvest stages (Ma et al., 2013). In northeastern Thailand, capillary rise from deeper layers in the dry season provided large amounts of water for evapotranspiration from the 0.5 m layer (Watanabe et al., 2004).

Deep percolation at the most representative location of the spatial mean SWS for the 0–1 m layer well estimated the spatial mean deep percolation below a depth of 2 m, with high R^2 and near-zero MARE in the northern and southern croplands (Fig. 8). The prediction accuracies, however, were low, especially in the southern cropland. Capillary rise occasionally occurred at some locations in the southern cropland during the measurement period, which significantly impacted the spatial mean deep percolation.

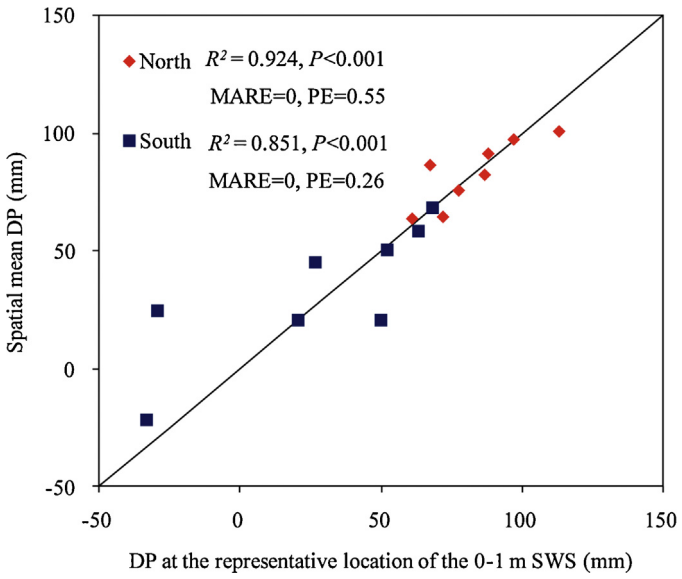

Fig. 8. The comparison of deep percolation at the most representative location of spatial mean soil water storage in the 0–1 m layer to the spatial mean deep percolation in the northern and southern croplands.

Nevertheless, the future management of agricultural water can be generally based on the measurements of meteorological variables and SWS at the four representative locations. Once the feasibility of this approach is verified by measurement over a longer term, it may provide information for determining water-conserving irrigation schedules for large-scale arid regions in northwestern China. The existing efficiency of irrigation is low in the study area, and measures should be taken to reduce the deep percolation after irrigation. An irrigation schedule with more frequent applications and lower amounts may be more suitable (Ji et al., 2007). Advanced irrigation technologies should be encouraged, such as pulse-drip and sprinkler irrigation.

4. Conclusions

Two irrigated croplands for the production of maize seeds in an arid region of northwestern China were selected to evaluate the temporal variation of components of the soil water balance. Meteorological factors were monitored in the study area in 2011 and 2012, and SWS profiles (0–1 and 1–2 m layers) were determined over 18 occasions from 31 and 17 locations in the northern and southern croplands, respectively. Crop evapotranspiration, SWS variation and deep percolation were analyzed during the maize growing periods. Soil water storages in the 0–1 and 1–2 m soil layers of the northern and southern croplands were temporally stable. The location with the lowest standard deviation of relative differences after offset could accurately estimate the spatial mean SWS and was identified as the most representative location. The most representative locations for the 0–1 m layer could generally represent SWS in the 0–2 m soil profile in both croplands. Deep percolation from 21 May to late September represented ~39 and 22% of the irrigation and rainfall in the northern and southern croplands, respectively. These different percentages for the same period may be ascribed to a delay of the growing season in the southern cropland and to differences in water-holding capacity. Deep percolation was high in the initial, development and senescence stages. Deep percolation at the most representative locations of spatial mean SWS for the 0–1 m layers was generally able to estimate the spatial mean deep percolation below a depth of 2 m. Measurements over a longer term are needed to verify the feasibility of predicting the spatial mean SWS and deep percolation from the representative locations. The results of this study may have implications for determining a water-conserving irrigation schedule in arid regions of northwestern China.

Acknowledgements

This study was financially supported by the National Natural Science Foundation of China (91025018). Authors appreciate the Linze Inland River Basin Comprehensive Research Station, Chinese Ecosystem Research Network, for providing the meteorological data. Sincere thanks go to the editor and the anonymous reviewer for their useful comments and suggestion, which greatly helped us to improve this manuscript.

References

Allen, R.G., Pereira, L.S., Raes, D., Smith, M., 1998. Crop Evapotranspiration – Guidelines for Computing Crop Water Requirements. FAO Irrigation and Drainage paper 56. FAO, Rome.
Chang, X.X., Zhao, W.Z., Zhang, Z.H., Su, Y.Z., 2006. Sap flow and tree conductance of shelter-belt in arid region of China. Agric. Forest Meteorol. 138, 132–141.
Chen, D.J., Xu, Z.M., Chen, R.S., 2003. Design of water resources accounts: a case of integrated environmental and economic accounting. Adv. Water Sci. 14, 631–637.
Chen, Y., Zhang, D.Q., Sun, Y.B., Liu, X.A., Wang, N.Z., Savenije, H.H.G., 2005. Water demand management: a case study of the Heihe River Basin in China. Phys. Chem. Earth 30, 408–419.
Choi, M., Jacobs, J.M., 2007. Soil moisture variability of root zone profiles within SMEX02 remote sensing footprints. Adv. Water Resour. 30, 883–896.
Cosh, M.H., Jackson, T.J., Moran, S., Bindlish, R., 2008. Temporal persistence and stability of surface soil moisture in a semi-arid watershed. Remote Sens. Environ. 112, 304–313.
Cosh, M.H., Evett, S.R., McKee, L., 2012. Surface soil water content spatial organization within irrigated and non-irrigated agricultural fields. Adv. Water Resour. 50, 55–61.
de Souza, E.R., Montenegro, A.A.D.A., Montenegro, S.M.G., de Matos, J.D.A., 2011. Temporal stability of soil moisture in irrigated carrot crops in Northeast Brazil. Agric. Water Manage. 99, 26–32.
Grayson, R.B., Western, A.W., 1998. Towards areal estimation of soil water content from point measurements: time and space stability of mean response. J. Hydrol. 207, 68–82.
Guber, A.K., Gish, T.J., Pachepsky, Y.A., van Genuchten, M.T., Daughtry, C.S.T., Nicholson, T.J., Cady, R.E., 2008. Temporal stability in soil water content patterns across agricultural fields. Catena 73, 125–133.
Hu, W., Shao, M.A., Han, F.P., Reichardt, K., Tan, J., 2010a. Watershed scale temporal stability of soil water content. Geoderma 158, 181–198.
Hu, W., Shao, M.A., Reichardt, K., 2010b. Using a new criterion to identify sites for mean soil water storage evaluation. Soil Sci. Soc. Am. J. 74, 762–773.
Hu, W., Shao, M.A., Si, B.C., 2012a. Seasonal changes in surface bulk density and saturated hydraulic conductivity of natural landscapes. Eur. J. Soil Sci. 63, 820–830.
Hu, W., Tallon, L.K., Si, B.C., 2012b. Evaluation of time stability indices for soil water storage upscaling. J. Hydrol. 475, 229–241.
Hu, W., Biswas, A., Si, B.C., 2014. Application of multivariate empirical mode decomposition for revealing scale-and season-specific time stability of soil water storage. Catena 113, 377–385.
Hu, W., Si, B.C., 2014. Can soil water measurements at a certain depth be used to estimate mean soil water content of a soil profile at a point or at a hillslope scale? J. Hydrol., http://dx.doi.org/10.1016/j.jhydrol.2014.01.053.
Jacobs, J.M., Mohanty, B.P., Hsu, E.C., Miller, D., 2004. SMEX02: field scale variability, time stability and similarity of soil moisture. Remote Sens. Environ. 92, 436–446.
Ji, X.B., Kang, E.S., Chen, R.S., Zhao, W.Z., Zhang, Z.H., Jin, B.W., 2007. A mathematical model for simulating water balances in cropped sandy soil with conventional flood irrigation applied. Agric. Water Manage. 87, 337–346.
Jiménez-Martínez, J., Skaggs, T.H., van Genuchten, M.Th., Candela, L., 2009. A root zone modelling approach to estimating groundwater recharge from irrigated areas. J. Hydrol. 367, 138–149.
Kang, Y.H., Wang, R.S., Wan, S.Q., Hu, W., Jiang, S.F., Liu, S.P., 2012. Effects of different water levels on cotton growth and water use through drip irrigation in an arid region with saline ground water of Northwest China. Agric. Water Manage. 109, 117–126.
Klute, A., Dirksen, C., 1986. Hydraulic conductivity of saturated soils. In: Klute, A. (Ed.), Methods of Soil Analysis. ASA and SSSA, Madison, Wisconsin, USA, pp. 694–700.
Li, D.F., Shao, M.A., 2013. Simulating the vertical transition of soil textural layers in north-western China with a Markov chain model. Soil Res. 51, 182–192.
Li, D.F., Shao, M.A., 2014. Soil organic carbon and influencing factors in different landscapes in an arid region of northwestern China. Catena 116, 95–104.
Li, Y.L., Cui, J.Y., Zhang, T.H., Zhao, H.L., 2003. Measurement of evapotranspiration of irrigated spring wheat and maize in a semi-arid region of north China. Agric. Water Manage. 61, 1–12.

Liu, B., Zhao, W.Z., Chang, X.X., Li, S.B., Zhang, Z.H., Du, M.W., 2010. Water requirements and stability of oasis ecosystem in arid region, China. Environ. Earth Sci. 59, 1235–1244.
Liu, J.M., An, S.Q., Liao, R.W., Ren, S.X., Liang, H., 2009. Temporal variation and spatial distribution of the root system of corn in a soil profile. Chin. J. Eco-Agric. 17, 517–521 (in Chinese with English abstract).
Ma, Y., Feng, S.Y., Song, X.F., 2013. A root zone model for estimating soil water balance and crop yield responses to deficit irrigation in the North China Plain. Agric. Water Manage. 127, 13–24.
Martínez-Fernández, J., Ceballos, A., 2003. Temporal stability of soil moisture in a large-field experiment in Spain. Soil Sci. Soc. Am. J. 67, 1647–1656.
Martinez, G., Pachepsky, Y.A., Vereecken, H., Hardelauf, H., Herbst, M., Vanderlinden, K., 2013. Modeling local control effects on the temporal stability of soil water content. J. Hydrol. 481, 106–118.
Moreno, F., Cayuela, J.A., Fernández, J.E., Fernández-Boy, E., Murillo, J.M., Cabrera, F., 1996. Water balance and nitrate leaching in an irrigated maize crop in SW Spain. Agric. Water Manage. 32, 71–83.
Pachepsky, Y.A., Guber, A.K., Jacques, D., 2005. Temporal persistence in vertical distributions of soil moisture contents. Soil Sci. Soc. Am. J. 69, 347–352.
Panigrahi, B., Panda, S.N., 2003. Field test of a soil water balance simulation model. Agric. Water Manage. 58, 223–240.
Penna, D., Brocca, L., Borga, M., Dalla Fontana, G.D., 2013. Soil moisture temporal stability at different depths on two alpine hillslopes during wet and dry periods. J. Hydrol. 477, 55–71.
Pereira, L.S., Goncalves, J.M., Dong, B., Mao, Z., Fang, S.X., 2007. Assessing basin irrigation and scheduling strategies for saving irrigation water and controlling salinity in the upper Yellow River Basin, China. Agric. Water Manage. 93, 109–122.
Schneider, K., Huisman, J.A., Breuer, L., Zhao, Y., Frede, H.G., 2008. Temporal stability of soil moisture in various semi-arid steppe ecosystems and its application in remote sensing. J. Hydrol. 359, 16–29.
Sella, B., Minasny, B., Bethune, M., Thayalakumaran, T., Chandra, S., 2011. Applicability of Richards' equation models to predict deep percolation under surface irrigation. Geoderma 160, 569–578.
Starks, P.J., Heathman, G.C., Jackson, T.J., Cosh, M.H., 2006. Temporal stability of soil moisture profile. J. Hydrol. 324, 400–411.
Starr, G.C., 2005. Assessing temporal stability and spatial variability of soil water patterns with implications for precision water management. Agric. Water Manage. 72, 223–243.
Stewart, L.K., Charlesworth, P.B., Bristow, K.L., Thorburn, P.J., 2006. Estimating deep drainage and nitrate leaching from the root zone under sugarcane using APSIM-SWIM. Agric. Water Manage. 81, 315–334.
Su, Y.Z., Liu, W.J., Yang, R., Chang, X.X., 2009. Changes in soil aggregate, carbon, and nitrogen storages following the conversion of cropland to alfalfa forage land in the marginal oasis of northwest China. Environ. Manage. 43, 1061–1070.
Su, Y.Z., Yang, R., Liu, W.J., Wang, X.F., 2010. Evolution of soil structure and fertility after conversion of native sandy desert soil to irrigated cropland in arid region, China. Soil Sci. 175, 246–254.
Tanji, K.K., Kielen, N.C., 2002. Agricultural drainage water management in arid and semi-arid areas. FAO Irrigation and Drainage Paper 61.
Teare, I.D., Peet, M.M., 1983. Crop–Water Relations. John Wiley & Sons, Michigan.
Vachaud, G., Passerat De Silans, A., Balabanis, P., Vauclin, M., 1985. Temporal stability of spatially measured soil water probability density function. Soil Sci. Soc. Am. J. 49, 822–828.
Van Pelt, R.S., Wierenga, P.J., 2001. Temporal stability of spatially measured soil matric potential probability density function. Soil Sci. Soc. Am. J. 65, 668–677.
Vanderlinden, K., Vereecken, H., Hardelauf, H., Herbst, M., Martinez, G., Cosh, M.H., Pachepsky, Y.A., 2012. Temporal stability of soil water contents: a review of data and analyses. Vadose Zone J., 11.
Vázquez, N., Pardo, A., Suso, M.L., Quemada, M., 2006. Drainage and nitrate leaching under processing tomato growth with drip irrigation and plastic mulching. Agric. Ecosyst. Environ. 112, 313–323.
Wang, G.X., Cheng, G.D., 1999. Water resource development and its influence on the environment in arid areas of China – the case of the Hei River basin. J. Arid Environ. 43, 121–131.
Wang, P., Song, X.F., Han, D.M., Zhang, Y.H., Zhang, B., 2012. Determination of evaporation, transpiration and deep percolation of summer corn and winter wheat after irrigation. Agric. Water Manage. 105, 32–37.
Watanabe, K., Yamamoto, T., Yamda, T., Sakuratani, T., Nawata, E., Noichana, C., Sributta, A., Higuchi, H., 2004. Changes in seasonal evapotranspiration, soil water content, and crop coefficients in sugarcane, cassava, and maize fields in Northeast Thailand. Agric. Water Manage. 67, 133–143.
Zhang, P.P., Shao, M.A., 2013. Temporal stability of surface soil moisture in a desert area of northwestern China. J. Hydrol. 505, 91–101.
Zhao, W.Z., Liu, B., Zhang, Z.H., 2010. Water requirements of maize in the middle Heihe River basin, China. Agric. Water Manage. 97, 215–223.
Zhou, S.L., Wu, Y.C., Wang, Z.M., Lu, L.Q., Wang, R.Z., 2008. The nitrate leached below maize root zone is available for deep-rooted wheat in winter wheat–summer maize rotation in the North China Plain. Environ. Pollut. 152, 723–730.